Non-Markovian dynamic evolution of spontaneous emission decay of a two-level atom embedded in one-dimensional photonic crystals

Nian-Hua Liu,[1,2] Jing-Ping Xu,[2,3] and Shi-Yao Zhu[1,2,3]
[1]*Department of Physics, Nanchang University, Nanchang 330047, China*
[2]*Department of Physics, Hong Kong Baptist University, Kowloon Tong, Hong Kong*
[3]*Department of Physics, Tongji University, Shanghai 200092, China*
(Received 5 March 2006; revised manuscript received 8 May 2006; published 11 August 2006)

The dynamic evolution of atomic spontaneous emission in one-dimensional photonic crystals (1DPC) is investigated by using mode functions for the 1DPC. Our attention is focused on the non-Markovian processes in the first several optical cycles of the spontaneous emission decay. The integral-differential dynamic equation is directly solved by numerical calculation without using the Markovian approximation. The interference of the multireflected fields plays an important role in the non-Markovian processes. Due to the interference of the fields successive arrived at the atom due to the reflection at the interfaces, the decay rate shows a series of pulselike peaks. If the interference is constructive, the spontaneous decay is enhanced, while if the interference is destructive, the spontaneous decay is suppressed. The steady decay rate is approximately equal to the vacuum decay rate, when the atomic transition frequency corresponds to an allowed normal mode of the 1DPC. The spontaneous emission decay is suppressed if the atomic transition frequency is within the forbidden gap of the 1DPC.

DOI: 10.1103/PhysRevB.74.075314 PACS number(s): 42.50.Ct, 42.25.Bs, 73.21.Ac, 42.70.Qs

I. INTRODUCTION

Spontaneous emission (SE) from an excited atom is a basic problem in quantum electrodynamics. According to the Weisskopf-Wigner theory, the spontaneous decay in the free space[1] is $\exp(-\Gamma_0 t)$, with the constant decay rate of Γ_0. The exponential decay law is a result of the Markovian approximation and is applicable after a long time compared with one optical period at the transition frequency. In the early stage of the spontaneous emission, however, there exist quantum Zeno effects or anti-Zeno effects, depending on the measurement.[2,3] The decay is not according to the exponential law. Consequently suppressed or accelerated decay can be achieved by frequent measurements. The nonexponential decay was as well as predicated under different theoretical models.[4,5]

The behavior of SE decay will be changed if the atom is put into different environments since there are different densities of modes which determine the SE decay rate. In 1987, Yablonovitch and John suggested the concept of photonic crystals,[6] which are wavelength-scale, periodic dielectric structures. In the photonic crystals, the optical modes exhibit a band-gap structure. If the frequency of the mode is located in the gap, the propagation is forbidden. Thus, the SE of an atom embedded in the photonic crystals is quite different from the SE in the vacuum[7–12] and depends on the structure of the photonic crystals.

The microcavity is an important structure for device application. The SE decay of atoms in the microcavity, particularly the planar microcavity, has been extensively studied.[13–21] A complete set of orthonormal-mode functions was derived for a sandwich structure of dielectric slabs,[14] and the SE decay rate for a two-level atom in the structure was investigated under the Markovian approximation. The effect of the multireflected fields in the Fabry-Perot (F-P) cavity on the SE rate was considered by Dutra and Knight.[15] A complete set of cavity modes including the guided modes was suggested.[16] It was demonstrated that a large amount of light is emitted into the guided modes. Based on the complete set of the mode functions, the atom-location-dependent SE intensity and the spectra for the *F-P* cavity were calculated with the nonperturbation theory.[17,18] The second quantization theory was extended to the field in the one-dimensional photonic crystals via a quasinormal-mode approach.[19] The optical power and the fields radiated by an oscillating dipole in layered structure were evaluated.[20] Recently, we have calculated the SE field of a two-level atom embedded in one-dimensional photonic crystals (1DPC), composed alternately of left-handed and right-handed material under the condition of impedance matching.[21] Most of the previous approaches for 1DPC were based on the Markovian approximation. In this paper, we consider the non-Markovian process of the SE decay of a two-level atom embedded in 1DPC. First, we define a complete set of optical mode functions for the 1DPC by using the complex reflection coefficients and the complex transmission coefficients. Next we construct a reservoir coupling spectrum with the mode functions. From the reservoir coupling spectrum we introduce a memory function for the non-Markovian process. The integral-differential dynamic equation is directly solved by numerical calculation. Our attention is focused on the early evolution of the SE decay in the first several optical cycles.

II. THE DYNAMIC EQUATION OF A TWO-LEVEL ATOM IN 1DPC

The structure under consideration is schematically shown in Fig. 1. The origin of the coordinator system is at the center of the structure. The z-axis is normal to the interface of the 1DPC. The refractive index, permittivity, permeability, and

 ©2006 The American Physical Society

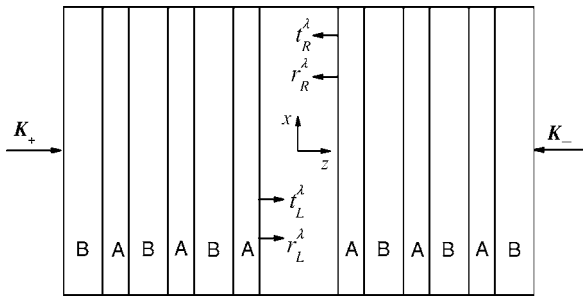

FIG. 1. Schematic view of the 1DPC structure.

thickness of layer A and layer B are indicated by $n_A, \varepsilon_A, \mu_A, d_A$ and $n_B, \varepsilon_B, \mu_B, d_B$, respectively. The middle layer with thickness d_0 is taken to be vacuum ($n_0=1$). Such a structure can be regarded as a finite 1DPC containing a defect layer, which is in fact a microcavity of multilayer mirrors. The two-level atom with dipole moment $\boldsymbol{p}$ is placed in the middle layer, and its position is at $\boldsymbol{r}_a=(0,0,z_a)$.

The positive frequency part of the electric field operator at the position of the atom is written as[21]

$$\boldsymbol{E}^{(+)}(\boldsymbol{r}_a,t)=\sum_{\boldsymbol{K}_+,\lambda} U(\boldsymbol{K}_+,\lambda,\boldsymbol{r}_a)\hat{\boldsymbol{e}}_+\xi_K a_{\boldsymbol{K}_+\lambda}e^{-i\omega_K t} + \sum_{\boldsymbol{K}_-,\lambda} U(\boldsymbol{K}_-,\lambda,\boldsymbol{r}_a)\hat{\boldsymbol{e}}_-\xi_K a_{\boldsymbol{K}_-\lambda}e^{-i\omega_K t}, \tag{1}$$

where $\xi_K=(\omega_K/2\varepsilon_0 V)^{1/2}$, with $\omega_K=c|\boldsymbol{K}_\pm|=cK$. The first term on the right-hand side of Eq. (1) represents the modes coming from the left free space, and the second term refers to the modes coming from the right free space. $U(\boldsymbol{K}_+,\lambda,\boldsymbol{r}_a)$ and $U(\boldsymbol{K}_-,\lambda,\boldsymbol{r}_a)$ are the mode functions, which are given by

$$U(\boldsymbol{K}_+,\lambda,\boldsymbol{r}_a)\hat{\boldsymbol{e}}_+ = t_L^\lambda e^{iK_z z_{-N-1}}[e^{i\boldsymbol{K}_+\cdot\boldsymbol{r}-iK_z z_{-1}}\hat{\boldsymbol{e}}(\boldsymbol{K}_+,\lambda) + r_R^\lambda e^{i\boldsymbol{K}_-\cdot\boldsymbol{r}+iK_z(z_{-1}+2d_0)}\hat{\boldsymbol{e}}(\boldsymbol{K}_-,\lambda)]/D^\lambda, \tag{2}$$

$$U(\boldsymbol{K}_-,\lambda,\boldsymbol{r}_a)\hat{\boldsymbol{e}}_- = t_R^\lambda e^{-iK_z z_N}[e^{i\boldsymbol{K}_-\cdot\boldsymbol{r}+iK_z z_0}\hat{\boldsymbol{e}}(\boldsymbol{K}_-,\lambda) + r_L^\lambda e^{i\boldsymbol{K}_{m+}\cdot\boldsymbol{r}+iK_z(2d_0-z_0)}\hat{\boldsymbol{e}}(\boldsymbol{K}_+,\lambda)]/D^\lambda. \tag{3}$$

The wave vectors $\boldsymbol{K}_+$ (from the left to the right) and $\boldsymbol{K}_-$ (from the right to the left), corresponding to the forward and backward propagations, respectively, are defined as

$$\boldsymbol{K}_\pm=(K_x,K_y,\pm K_z) = K(\sin\theta\cos\phi,\sin\theta\sin\phi,\pm\cos\theta) \quad \theta\in(0,\pi/2), \tag{4}$$

where θ is the angle between $\boldsymbol{K}_+$ and the z axis. The superscription $\lambda=TE$ or TM indicates two transverse polarization directions. The unit vectors of the two perpendicular polarizations are

$$\begin{cases}\hat{\boldsymbol{e}}(\boldsymbol{K}_\pm,\lambda=TE)=(\sin\phi,-\cos\phi,0),\\ \hat{\boldsymbol{e}}(\boldsymbol{K}_\pm,\lambda=TM)=(\cos\theta\cos\phi,\cos\theta\sin\phi,\mp\sin\theta).\end{cases} \tag{5}$$

$a_{\boldsymbol{K}_+\lambda}$ and $a_{\boldsymbol{K}_-\lambda}$ are the annihilation operator of the modes $U(\boldsymbol{K}_+,\lambda,\boldsymbol{r}_a)$ and $U(\boldsymbol{K}_-,\lambda,\boldsymbol{r}_a)$, respectively. In Eqs. (2) and (3), t_L^λ (t_R^λ) denotes the transmission coefficient through the left (right) part of the middle layer, and r_R^λ (r_L^λ) denotes the reflective coefficient on the right (left) interface of the middle layer. They are dependent on $\boldsymbol{K}_\pm$, λ, and the structure of the 1DPC. The factor D_λ originates from the multireflection in two interfaces of the middle layer, which is given by

$$D^\lambda = 1 - r_L^\lambda r_R^\lambda e^{2iKd_0\cos\theta}. \tag{6}$$

The interaction Hamiltonian in the interaction picture is given by

$$V_I(t) = -\boldsymbol{p}\cdot\boldsymbol{E} = \sum_{\boldsymbol{K}_+,\lambda}[g^\lambda_{\boldsymbol{K}_+}(\boldsymbol{r}_a)\sigma_+ a_{\boldsymbol{K}_+\lambda}e^{i(\omega_a-\omega_K)t}+H.C.] + \sum_{\boldsymbol{K}_-,\lambda}[g^\lambda_{\boldsymbol{K}_-}(\boldsymbol{r}_a)\sigma_+ a_{\boldsymbol{K}_-\lambda}e^{i(\omega_a-\omega_K)t}+H.C.], \tag{7}$$

where the coupling coefficients are

$$g^\lambda_{\boldsymbol{K}_+}(\boldsymbol{r}_a) = -\frac{\xi_K}{\hbar}(t_L^\lambda/D^\lambda)e^{i\boldsymbol{K}_+\cdot\boldsymbol{r}_a+iK(z_{-N-1}+d_0/2)\cos\theta} \times[\boldsymbol{p}\cdot\hat{\boldsymbol{e}}(\boldsymbol{K}_+,\lambda)+\boldsymbol{p}\cdot\hat{\boldsymbol{e}}(\boldsymbol{K}_-,\lambda)r_R^\lambda e^{-iK(2z_a-d_0)\cos\theta}], \tag{8}$$

$$g^\lambda_{\boldsymbol{K}_-}(\boldsymbol{r}_a) = -\frac{\xi^K}{\hbar}(t_R^\lambda/D^\lambda)e^{i\boldsymbol{K}_-\cdot\boldsymbol{r}_a+iK(d_0/2-z_N)\cos\theta} \times[\boldsymbol{p}\cdot\hat{\boldsymbol{e}}(\boldsymbol{K}_-,\lambda)+\boldsymbol{p}\cdot\hat{\boldsymbol{e}}(\boldsymbol{K}_+,\lambda)r_L^\lambda e^{iK(2z_a+d_0)\cos\theta}], \tag{9}$$

with ω_a the atomic transition frequency.

The state vector of the system can be expressed as

$$|\psi_I(t)\rangle = C_a(t)|a,0\rangle + \sum_{\boldsymbol{K}_+,\lambda} C_{b\boldsymbol{K}_+\lambda}(t)|b,1_{\boldsymbol{K}_+\lambda}\rangle + \sum_{\boldsymbol{K}_-,\lambda} C_{b\boldsymbol{K}_-\lambda}(t)|b,1_{\boldsymbol{K}_-\lambda}\rangle, \tag{10}$$

where the state $|a,0\rangle$ indicates the atom in the excited state and no photon, and $|b,1_{\boldsymbol{K}_\pm\lambda}\rangle$ indicates the atom in the ground state with a photon of $(\boldsymbol{K}_\pm,\lambda)$. We assume the atom is initially in the excited state and there is no photon, i.e., $C_a(0)=1$ and $C_{b\boldsymbol{K}_\pm\lambda}(0)=0$. From the Schrödinger equation we obtain the atomic dynamical equations,

$$\frac{dC_a(t)}{dt} = -i\sum_{\boldsymbol{K}_+,\lambda} g^\lambda_{\boldsymbol{K}_+}(\boldsymbol{r}_a)C_{b\boldsymbol{K}_+\lambda}(t)e^{i(\omega_a-\omega_K)t} - i\sum_{\boldsymbol{K}_-,\lambda} g^\lambda_{\boldsymbol{K}_-}(\boldsymbol{r}_a)C_{b\boldsymbol{K}_-\lambda}(t)e^{i(\omega_a-\omega_K)t}, \tag{11}$$

$$\frac{dC_{b\boldsymbol{K}_+\lambda}(t)}{dt} = -i[g^\lambda_{\boldsymbol{K}_+}(\boldsymbol{r}_a)]^* e^{-i(\omega_a-\omega_K)t}C_a(t), \tag{12}$$

$$\frac{dC_{b\boldsymbol{K}_-\lambda}(t)}{dt} = -i[g^\lambda_{\boldsymbol{K}_-}(\boldsymbol{r}_a)]^* e^{-i(\omega_a-\omega_K)t}C_a(t). \tag{13}$$

The summarization over $\boldsymbol{K}_+$ and $\boldsymbol{K}_-$ can be changed to the integral

$$\sum_{\boldsymbol{K}_\pm} \to \frac{V}{(2\pi)^3}\int d\boldsymbol{K}_\pm = \frac{V}{(2\pi)^3}\int_0^\infty dK \int_0^{\pi/2} d\theta \int_0^{2\pi} d\phi K^2 \sin\theta. \tag{14}$$

Integrating Eqs. (12) and (13) over time, and substituting them into (11), we have

$$\frac{dC_a(t)}{dt} = -\frac{V}{(2\pi)^3} \times \int_0^t dt' \int_0^\infty dK K^2 \int_0^{2\pi} d\phi \int_0^{\pi/2} d\theta \sin\theta \times \sum_{\lambda=1}^{2} [|g^\lambda_{\boldsymbol{K}_+}(\boldsymbol{r}_a)|^2 + |g^\lambda_{\boldsymbol{K}_-}(\boldsymbol{r}_a)|^2] e^{ic(k-K)(t-t')} C_a(t'), \tag{15}$$

where $k=\omega_a/c$ and $K=\omega_K/c$. Then Eq. (15) can be rewritten as

$$\frac{dC_a(t)}{dt} = -\frac{\Gamma_0}{2\pi}\int_0^t d\tau \int_0^\infty d\omega_K f(\omega_K) e^{i(\omega_a-\omega_K)(t-\tau)} C_a(\tau), \tag{16}$$

where $\Gamma_0=p^2k^3/(3\pi\varepsilon_0\hbar)$ is the decay rate in the free space, and $f(\omega_K)$ is the reservoir coupling spectrum, which is determined by the coupling of the atom to the field. In our model, it is given by

$$f(\omega_K) = \frac{V\omega_K^2}{\Gamma_0(2\pi)^2c^3}\int_0^{\pi/2} d\theta \int_0^{2\pi} d\phi \sin\theta \times \sum_{\lambda=1}^{2} [|g^\lambda_{\boldsymbol{K}_+}(\boldsymbol{r}_a)|^2 + |g^\lambda_{\boldsymbol{K}_-}(\boldsymbol{r}_a)|^2]. \tag{17}$$

Obviously, the integration of $f(\omega_K)$ over frequency ω_K is divergent, because $f(\omega_K)$ is proportional to ω_K^3 when $\omega_K \to \infty$. (Note that $|g^\lambda_{\boldsymbol{K}_\pm}(\boldsymbol{r}_a)|^2$ contains $|\xi_K|^2$, which contributes a ω_K.) The problem originates from the coupling constants, where all modes including infinitely high frequencies are taken into account with the same weight. From the point of physical view, there is an up-limitation on the frequency for the interaction between the atom and the modes, which is limited by the mass-energy relation, $m_ec^2=\omega_{\max}$. Taking into account this limitation, we assume that the coupling of the modes to the atom have a weight factor,[2]

$$w(\omega_K) = \frac{1}{[1+(\omega_K/\omega_B)^2]^2}, \tag{18}$$

where $\omega_B \approx c/a_B$ is the nonrelativistic cutoff frequency,[2] with a_B as the radius of the electron orbit. In general, ω_B has the magnitude order of $10^{17}\sim 10^{18}$ Hz ($\omega_B \gg \omega_a$), depending on the atom.

Multiplying the weight factor $w(\omega_K)$ to the coupling coefficients $g^\lambda_{\boldsymbol{K}_+}(\boldsymbol{r}_a)$ in Eq. (8) and $g^\lambda_{\boldsymbol{K}_-}(\boldsymbol{r}_a)$ in Eq. (9), we have the modified coupling spectrum function

$$f(\omega_K) = \frac{V\omega_K^2}{\Gamma_0(2\pi)c^3}\frac{1}{[1+(\omega_K/\omega_B)^2]^4}\int_0^{\pi/2} d\theta \sin\theta \times \sum_{\lambda=1}^{2} [|g^\lambda_{\boldsymbol{K}_+}(\boldsymbol{r}_a)|^2 + |g^\lambda_{\boldsymbol{K}_-}(\boldsymbol{r}_a)|^2]. \tag{19}$$

Substituting the coupling coefficients (8) and (9) into Eq. (19), the coupling spectrum function can be written as

$$f(\omega_K) = f_v(\omega_K) f_m(\omega_K), \tag{20}$$

where

$$f_v(\omega_K) = \frac{(\omega_K/\omega_a)^3}{[1+(\omega_K/\omega_B)^2]^4} \tag{21}$$

is the coupling spectrum function of free space. For the atomic dipole moment along the x axis, $\boldsymbol{p}=p(1,0,0)$, we have

$$f_m(\omega_K) = (3/8)\int_0^{\pi/2} d\theta \sin\theta \left\{ \left(\frac{1-|r_L^{TE}|^2}{|D^{TE}|^2}|1+r_R^{TE}e^{i(\omega_K/c)(d_0-2z_a)\cos\theta}|^2 + \frac{1-|r_R^{TE}|^2}{|D^{TE}|^2}|1+r_L^{TE}e^{i(\omega_K/c)(d_0+2z_a)\cos\theta}|^2 \right) + \cos^2\theta \left(\frac{1-|r_L^{TM}|^2}{|D^{TM}|^2}|1+r_R^{TM}e^{i(\omega_K/c)(d_0-2z_a)\cos\theta}|^2 + \frac{1-|r_R^{TM}|^2}{|D^{TM}|^2}|1+r_L^{TM}e^{i\omega_K/c(d_0+2z_a)\cos\theta}|^2 \right) \right\}, \tag{22}$$

where the reflection coefficients r^{TE} and r^{TM} can be calculated layer by layer. The recursion relation is

$$r_i = \frac{r_{i\to i+1} + r_{i+1}e^{ik_{(i+1)}d_{(i+1)}\cos\theta_{(i+1)}}}{1 + r_{i\to i+1}r_{i+1}e^{ik_{(i+1)}d_{(i+1)}\cos\theta_{(i+1)}}}, \tag{23}$$

where $r_{i\to i+1}$ is the Fresnel reflective coefficient on the interface between the ith layer and the $(i+1)$-th layer, and

$$r^{TE}_{A\to B} = \frac{1-\alpha_{AB}\beta_{AB}}{1+\alpha_{AB}\beta_{AB}}, \tag{24}$$

$$r^{TM}_{A\to B} = \frac{\alpha_{AB}-\beta_{AB}}{\alpha_{AB}+\beta_{AB}}, \tag{25}$$

where

$$\alpha_{AB} = \frac{\cos\theta_B}{\cos\theta_A}, \tag{26}$$

$$\beta_{AB} = \frac{n_B/n_A}{\mu_B/\mu_A} = \frac{\sqrt{\varepsilon_B}\sqrt{\mu_B}/\sqrt{\varepsilon_A}\sqrt{\mu_A}}{\mu_B/\mu_A}. \tag{27}$$

If we let $x=t-\tau$, and define

$$F(x) = \frac{1}{\pi}\int_0^\infty d\omega_K e^{-i(\omega_K-\omega_a)x} f(\omega_K) = \frac{e^{i\omega_a x}}{\pi}\int_0^\infty d\omega_K e^{-i\omega_K x} f(\omega_K), \tag{28}$$

we get the dynamic equation of the SE decay,

$$\frac{dC_a(t)}{dt} = -\frac{\Gamma_0}{2}\int_0^t dx F(x) C_a(t-x). \tag{29}$$

From Eq. (29) we see that $F(x)$ has the meaning of "memory" function in the non-Markovian processes. Its extension in the time domain measures the memory time. Equations (28) implies that $F(x)$ is related to the inverse Fourier transform of the spectrum function $f(\omega_K)$. The wider the spectrum (white noise) is, the shorter the memory time.

We rewrite Eq. (29) in the form

$$\frac{dC_a(t)}{dt} = -\frac{\tilde{\Gamma}(t)}{2} C_a(t), \tag{30}$$

where

$$\tilde{\Gamma}(t) = \frac{\Gamma_0}{C_a(t)}\int_0^t dx F(x) C_a(t-x). \tag{31}$$

The time-dependent instantaneous decay rate can be obtained from

$$\Gamma(t) = \mathrm{Re}[\tilde{\Gamma}(t)]. \tag{32}$$

If we let the contribution of all the modes the same (the Weisskopf-Wigner approximation), i.e., $\omega_K=\omega_a$ and $\omega_B\to\infty$ (white noise), we have $f(\omega_K)\approx f_m(\omega_a)$ and

$$F(x) = \frac{e^{i\omega_a x}}{\pi}\int_0^\infty d\omega_K e^{-i\omega_K x} f_m(\omega_a) = f_m(\omega_a) e^{i\omega_a x}\left[\delta(x) - P\frac{i\pi}{x}\right]. \tag{33}$$

The first term of the memory function $F(x)$ in Eq. (33) is proportional to $\delta(x)$, that is to say, there is no memory time. Substitute Eq. (34) into (31) we find the decay rate is reduced to $\Gamma(t)=f_m(\omega_a)\Gamma_0=$constant, the result of the Markovian approximation. The second term is related to the Lamb shift.

Since $f(\omega_K)$ is convergent, it is possible to solve the dynamic equation (29) numerically. Here we would like to emphasize that although the structure is one-dimensional, the emission is still in three dimensions (all directions). By numerically integrating Eq. (29), we can get the time-dependent instantaneous decay rate and the evolution of the atom.

III. NON-MARKOVIAN PROCESSES OF SPONTANEOUS DECAY IN FREE SPACE

First, we consider the non-Markovian spontaneous emission decay of an atom in free space.[2] The reservoir coupling spectrum for the free space is simply given by $f(\omega_K)=f_v(\omega_K)$. The decay rates are shown in Fig. 2 for (a) $\omega_B/\omega_a=10$, (b) $\omega_B/\omega_a=100$, and (c) $\omega_B/\omega_a=1000$, respectively. The general behavior of the decay is that $\Gamma(t)$ increases initially from zero to a maximum, and approaches finally to a steady decay of $\Gamma(t)\approx\Gamma_0 f(\omega_a)$. Here we would like to emphasize that the time to reach steady state (constant decay rate Γ_0) is almost the same for any ω_B, which is about one optical cycle.

In order to investigate how the reservoir coupling spectrum affects the SE decay, we suppose that in the early stage of the decay (in the first several optical cycles), $C_a(t)$ is a slowly varying function, so that in Eq. (31) $C_a(t-x)\approx C_a(t)$, then

$$\tilde{\Gamma}(t) = \Gamma_0\int_0^t dx F(x). \tag{34}$$

Substituting (28) into (34) we have

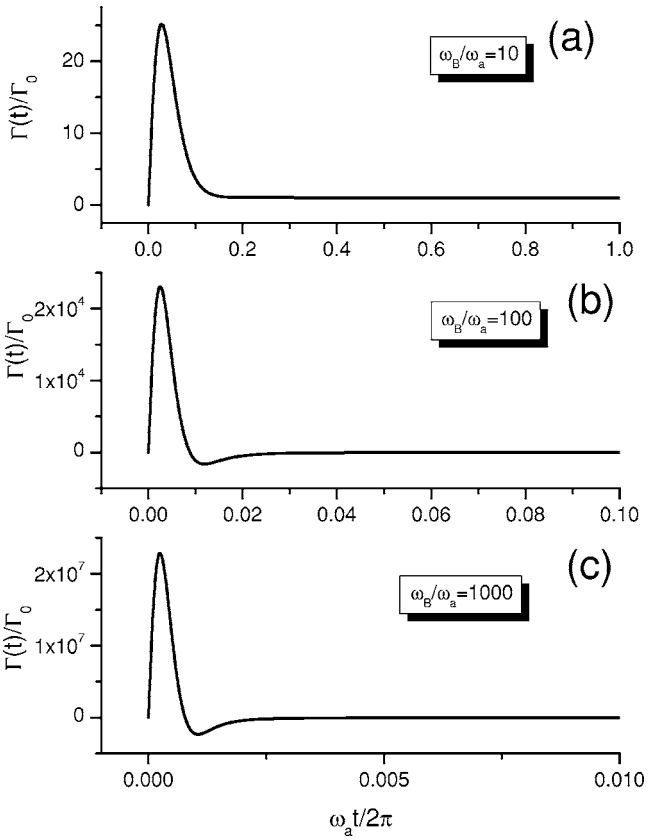

FIG. 2. SE decay rates in free space for (a) $\omega_B/\omega_a=10$, (b) $\omega_B/\omega_a=100$, and (c) $\omega_B/\omega_a=1000$, respectively.

$$\tilde{\Gamma}(t) = \frac{\Gamma_0}{\pi}\int_0^t dx \int_0^\infty d\omega_K e^{-i(\omega_K-\omega_a)x} f(\omega_K)$$

$$= \frac{\Gamma_0}{\pi}\int_0^\infty d\omega_K f(\omega_K)\frac{\sin[(\omega_K-\omega_a)t/2]}{(\omega_K-\omega_a)/2} e^{-i(\omega_K-\omega_a)t/2}. \quad (35)$$

Due to the sinc function $\{\sin[(\omega_K-\omega_a)t/2]/(\omega_K-\omega_a)/2\}$ in the integral, the main contribution of the reservoir coupling spectrum comes from the frequency region of $|(\omega_K-\omega_a)t/2| \leqslant \pi$. When t is small, a wide range of the reservoir coupling spectrum has contribution to the SE decay.

IV. SPONTANEOUS DECAY IN 1DPC

If the atom is placed in 1DPC, it will interact with the optical modes given by Eqs. (2) and (3). The only difference between the atom in the 1DPC and in the free space is the reservoir coupling spectrum $f(\omega_K)$. All information of the 1DPC is contained in $f_m(\omega_K)$, including the amplitude and phase of the reflected field from all interfaces back to the atom. The relative phase shifts from the atom to all interfaces are important because they determine the interference of the reflected fields at the atom. The memory function $F(x)$ is dependent on $f(\omega_K)$. From the dynamic equation (29) we see that the atomic evolution is determined by $F(x)$. Due to the change in $F(x)$, the atomic evolution in the 1DPC is quite different from that in the free space.

Since the typical size of the 1DPC is of the magnitude of wave length, the decay behavior in the early several optical cycles will be significantly influenced. The value of ω_B only influences the decay in the time interval $0<t<1/\omega_B$. The behavior in $t\sim 1/\omega_a$ is not sensitive to the value ω_B as long as $\omega_B \gg \omega_a$, so we choose $\omega_B/\omega_a=100$ in this paper (see Fig. 2).

First, we consider a 1DPC structure of $|B|A|B|A|B|A|0|A|B|A|B|A|B|$ with

$$\varepsilon_A = 4.0, \quad \mu_A = 1.0, \quad \varepsilon_B = 2.0, \quad \mu_B = 1.0,$$

$$d_0 = 0.5\lambda_a, \quad n_A d_A = n_B d_B = 0.25\lambda_a \quad (36)$$

where $\lambda_a=2\pi c/\omega_a$. The middle defect layer takes the role of a half-wave-length microcavity. Such a structure supports a normal defect mode of frequency ω_a. We assume the atom is placed at the center of the middle layer, the distance from the atom to the first interface is $\lambda_a/4$, and the time of the reflected field back to the atom after the first normal reflection is $t=\tau_0/2$, a half of the optical cycle, which corresponds to a phase shift of π. In addition to the "half-wave loss" on the interfaces, the total phase shifts from the interfaces back to the atom are 2π multiplied by integers, so that the reflected field has a constructive interference with the forward field, which results in a sudden enhancement of the interaction of the atom with the field and accelerates the decay with a pulselike peak in $\Gamma(t)$, as shown in Fig. 3. The second pulselike peak occurs when $t=2\times(\tau_0/2)$. It is the arrival time that the field reflected twice from the first interface. With time increases, a number of pulselike peaks appear in the decay

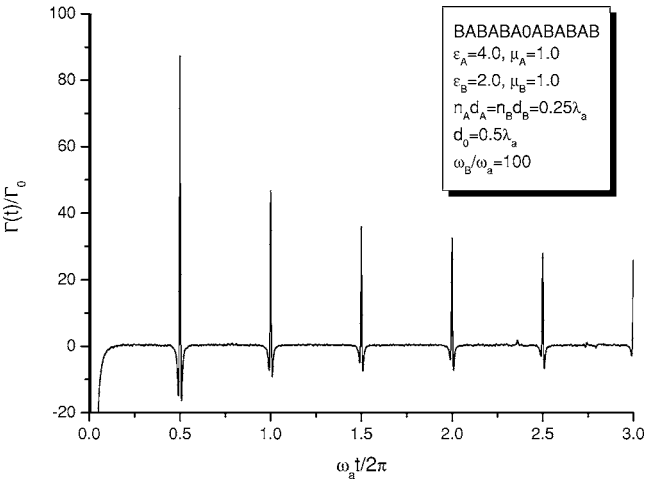

FIG. 3. SE decay rate in 1DPC with $\varepsilon_A=4.0$, $\mu_A=1.0$, $\varepsilon_B=2.0$, $\mu_B=1.0$, $d_0=0.5\lambda_a$, and $n_Ad_A=n_Bd_B=0.25\lambda_a$.

rate at $t=n\tau_0/2$ $(n=1,2,3)$. It should be noted that for other frequencies different from ω_a, the time $t=\tau_0/2$ is not a half of the optical cycle. Since all modes with different frequencies and different directions have interaction with the atom, the coupling of the atom to the field is very complicated. The complicated interaction leads to the oscillations of $\Gamma(t)$ around the peaks at $t=n\tau_0/2$. The evolution of $|C_a(t)|^2$ is shown in Fig. 4. We see that there are corresponding sudden changes at the time $t=n\tau_0/2$.

In the early stage of the SE decay, the dynamic evolution of $|C_a(t)|^2$ in the 1DPC is almost the same as in the free space. With time t increasing, their evolution behaviors become different. As we have discussed in the last section, the temporal evolution is dependent on the memory function $F(x)$, which is determined by the reservoir coupling spectrum $f(\omega_K)$. We have plotted the difference of the reservoir coupling spectra $\Delta f(\omega_K)=f(\omega_K)-f_v(\omega_K)$ in Fig. 5. The inset in Fig. 5 is the reservoir coupling spectrum $f_v(\omega_K)$ for the free space.

As mentioned in the last section, the frequency region which takes effect on the evolution is within $|(\omega_K-\omega_a)|$

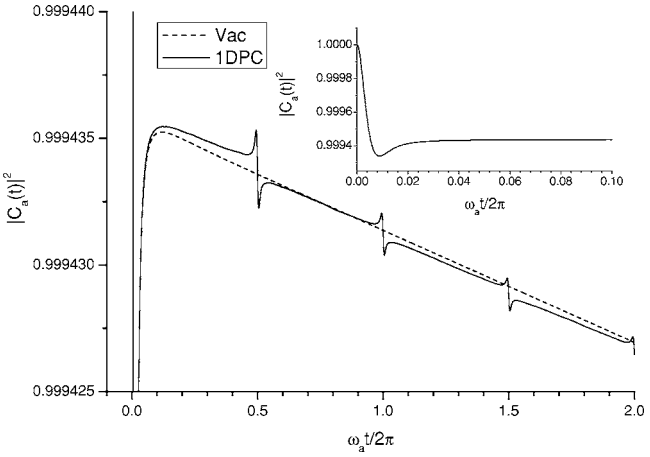

FIG. 4. Comparison of the evolutions of $|C_a(t)|^2$ in the 1DPC and in the free space.

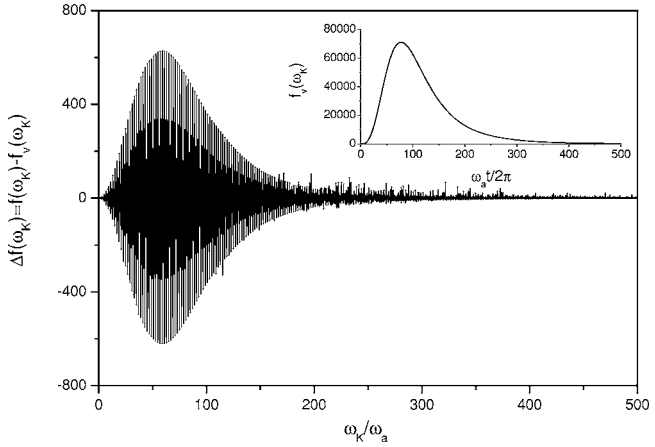

FIG. 5. The difference of the reservoir coupling spectra $\Delta f(\omega_K)=f(\omega_K)-f_v(\omega_K)$. Insert: The reservoir coupling spectrum for the free space $f_v(\omega_K)$.

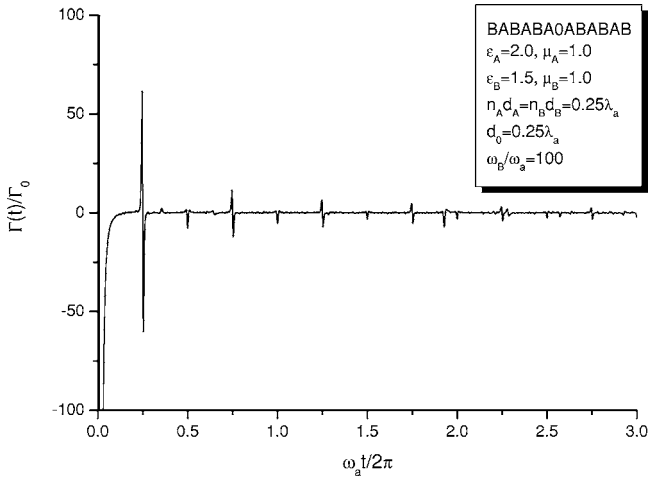

FIG. 6. SE decay rate in 1DPC with $\varepsilon_A=2.0$, $\mu_A=1.0$, $\varepsilon_B=1.5$, $\mu_B=1.0$, $d_0=\lambda_a/4$, and $n_Ad_A=n_Bd_B=\lambda_a/4$.

$\leqslant 2\pi/t$. The main contribution comes from the normal modes around the frequency ω_a. When t is small, almost the whole spectrum of $f(\omega_K)$ has influence on the evolution. From Eq. (28) we see when $t\to 0$, the memory function $F(x)\to F(0)=(1/\pi)\int_0^\infty d\omega_K f(\omega_K)$, which is simply proportional to the area under the curve of the reservoir coupling spectrum $f(\omega_K)$. Because $\Delta f(\omega_K)$ is an oscillatory function around 0 and $\Delta f(\omega_K)\ll f_v(\omega_K)$, as shown in Fig. 5, the area under the curve of $f(\omega_K)$ is approximately equal to the area under the curve of $f_v(\omega_K)$. Thus, the evolution in the 1DPC and the evolution in the free space are almost the same in the very early stage of $t\ll\tau_0$.

It is found that in the frequency interval of $|(\omega_K-\omega_a)|\leqslant 10/\tau_0$, the curves $f(\omega_K)$ and $f_v(\omega_K)$ have a larger difference, which leads to the change of the evolution in the time domain at about $t\approx 0.1\tau_0$. Since the typical size of the 1DPC is about $\lambda_a=2\pi c/\omega_a$, the geometry structure of the 1DPC influences significantly the spectrum of $f(\omega_K)$ at around ω_a. When t increases from zero to the magnitude around τ_0, the effective frequency region is in an interval around ω_a (from $0.1\omega_a$ to $200\omega_a$), where $f(\omega_K)$ and $f_v(\omega_K)$ are quite different. Consequently, the evolution in the 1DPC becomes different from that in the free space. There is pulselike evolution behavior at $t=n\tau_0/2$. When $t\to\infty$, the SE approaches to a steady decay, with the decay rate approaching $\Gamma_0 f(\omega_a)\approx\Gamma_0=$constant.

Next we consider a 1DPC which has the same structure as in Fig. 3, but the parameters are changed to the following,

$$\varepsilon_A=2.0,\quad \mu_A=1.0,\quad \varepsilon_B=1.5,\quad \mu_B=1.0,$$

$$d_0=0.25\lambda_a,\quad n_Ad_A=n_Bd_B=0.25\lambda_a. \tag{37}$$

In this case the middle layer has a thickness of a quarter-wave length. Thus, the structure is approximately regarded as a periodic structure. The frequency ω_a now is at the center of the band gap of the 1DPC, so that the interference of the reflection field is destructive. The evolution behavior of $\Gamma(t)$ is shown in Fig. 6. The reflected field comes to the atom at $t=\tau_0/4$ after the first normal reflection, which corresponds to a phase shift of $\pi/2$. In addition to the "half-wave loss" on the interfaces, the total phase shift of the field reflected from the interfaces back to the atom is an integral times of $3\pi/2$. When $t=\tau_0/4$, only the field reflected by the first interface comes to the atom. Due to the phase shift of $3\pi/2$, the superposition of the first arrival reflected field with the forward field causes to a sudden change in $\Gamma(t)$ at $t=\tau_0/4$. However, the superposition by more and more arrival fields with phase difference $n(3\pi/2)$ will cause the destructive interference. The destructive interference tends to suppress the interaction of the field with the atom. Thus, the peaks at $t=n\tau_0/4$ are different from those in Fig. 3.

It should be noted that in the present structure the optical thicknesses of all layers, including the middle layer, are the same. It can be approximately considered as a periodic structure. In the periodic media, as we know, a band gap for the modes is formed. The band gap is the result of the interference of the Bragg-reflected waves. In the periodic structure the phase shifts between two successive scattering points are the same. The special relation of the phase shifts may lead to the constructive interference or destructive interference, depending on the frequency of the multireflected waves. The constructive interference corresponds to the case that the frequency is within the passband. In this case the related field is an extended Bloch wave. However, for the destructive interference, the frequency is located in the gap region and the field is an evanescent wave. If the periodic structure is infinitely extended, then the evanescent wave in the frequency gap is completely suppressed, and the corresponding mode is completely forbidden. Since the present structure is almost periodic, the band-gap effect of the periodic structure becomes more evident. For the modes with certain wave-vector direction, the frequency may fall into the forbidden gap, but it may fall into the allowed band for another wave-vector direction. The coherent superposition of the multireflected fields may enhance or suppress the SE decay depending on the frequency and the wave-vector direction of the modes.

The corresponding evolution of $|C_a(t)|^2$ is shown in Fig. 7. In the very early stage, the evolutions in the 1DPC and in

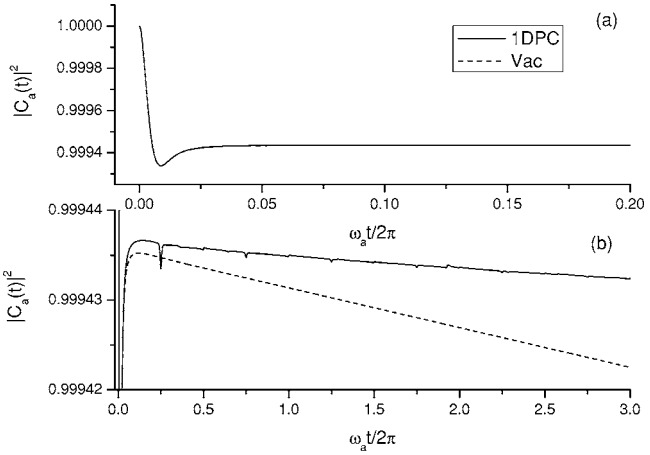

FIG. 7. Comparison of the evolutions of $|C_a(t)|^2$ in the 1DPC corresponding to Fig. 6 (solid line) and in the free space (dashed line). (a) In the very early stage, the evolutions are almost the same. (b) The difference of the evolutions in the 1DPC and in the free space.

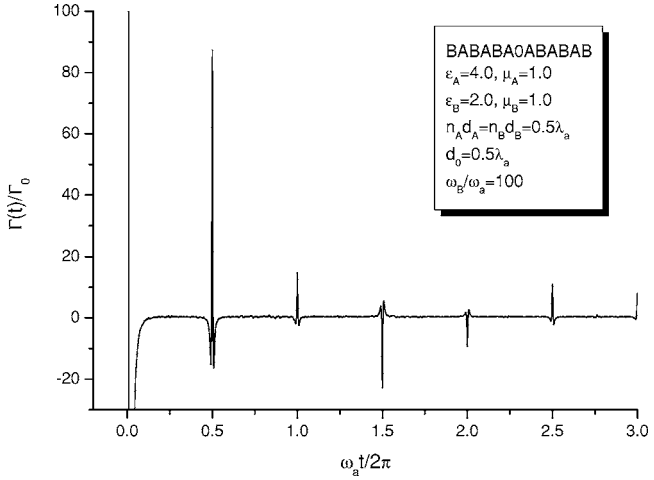

FIG. 8. SE decay rate in 1DPC with $\varepsilon_A=4.0$, $\mu_A=1.0$, $\varepsilon_B=2.0$, $\mu_B=1.0$, $d_0=\lambda_a/2$, and $n_A d_A=n_B d_B=\lambda_a/2$.

the free space are almost the same. With time increasing, they have different behaviors. When $t\to\infty$, the SE approaches to a steady decay with the decay rate approximately equal to $\Gamma_0 f(\omega_a)\approx 0.54\Gamma_0$, about half of the vacuum decay rate. This is different from the case in Fig. 3. In the structure of Fig. 3, the middle layer is a half-wave defect which supports a normal defect mode of frequency ω_a. The spontaneous emitted energy can be released through the defect mode to the out space. However, for the structure of Fig. 6, the frequency ω_a is in the forbidden gap. There is no normal mode to bridge the atom to the out space to release the spontaneous emitted energy. It is the forbidden gap of the photonic crystal that suppresses the spontaneous emission. Although the normal mode of frequency ω_a is forbidden in the 1DPC, there are still other modes with different direction and different frequency interacting with the atom. So the spontaneous emission is not completely inhibited.

Now we consider the case that the atomic transition frequency ω_a is located in the passband of the 1DPC. The parameters are taken as

$$\varepsilon_A = 4.0, \quad \mu_A = 1.0, \quad \varepsilon_B = 2.0, \quad \mu_B = 1.0,$$

$$n_0 d_0 = \lambda_a/2, \quad n_A d_A = n_B d_B = \lambda_a/2. \tag{38}$$

Instead of the quarter-wave stack as in the above two cases, here the 1DPC is a half-wave stack. Hence, the frequency ω_a is located in the center of the second passband. The evolution of the decay rate is shown in Fig. 8, and the evolution of $|C_a(t)|^2$ is shown in Fig. 9. We have also seen the pulselike behavior of the decay at the time $t=n\tau_0/2$. Since such a structure is almost a periodic structure, the band-gap structure exists for all directions, although the gap frequency interval may vary with the direction. The SE decay is therefore influenced by the band-gap effect. The coherent superposition of the multireflected fields with different frequencies and different directions may result in the constructive interference or destructive interference. For example, at $t=\tau_0/2$, the normal reflected field from the *first* interface makes a positive contribution to the decay. But at $t=3\tau_0/2$, the normal reflected field from the *second* interface makes an opposite contribution to the SE decay, which drives the atom from the lower level back to the higher level, as shown by the negative peak of the decay rate at $t=3\tau_0/2$, due to the suitable phase coherence of the atom with the field. Since the frequency ω_a is in the passband, the steady decay rate is larger than that in Fig. 6. At $t\to\infty$, the decay rate is approximately equal to $\Gamma_0 f(\omega_a)\approx 0.95\Gamma_0$.

In Fig. 10, we show the SE decay rate for $d_0=\lambda_a/8$, a very thin middle layer. The other parameters are the same as in Fig. 3. The corresponding evolution of $|C_a(t)|^2$ is shown in Fig. 11. It is found that the SE decay rate has a large sudden change with $\Gamma(t)/\Gamma_0$, dropping to -300 at $t=\tau_0/8$. In addition to the half-wave loss on the first interface, the total phase shift is $5\pi/4$. A larger change of $|C_a(t)|^2$ is found at this time. The effect of the interference of the multireflected

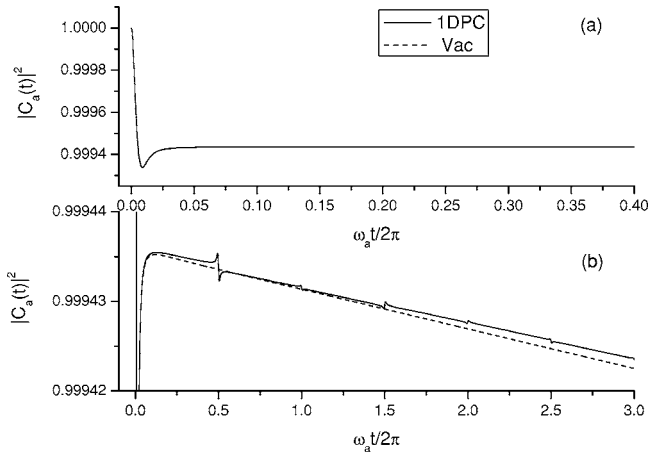

FIG. 9. Comparison of the evolutions of $|C_a(t)|^2$ in the 1DPC corresponding to Fig. 8 (solid line) and in the free space (dashed line). (a) In the very early stage, the evolutions are almost the same. (b) The difference of the evolutions in the 1DPC and in the free space.

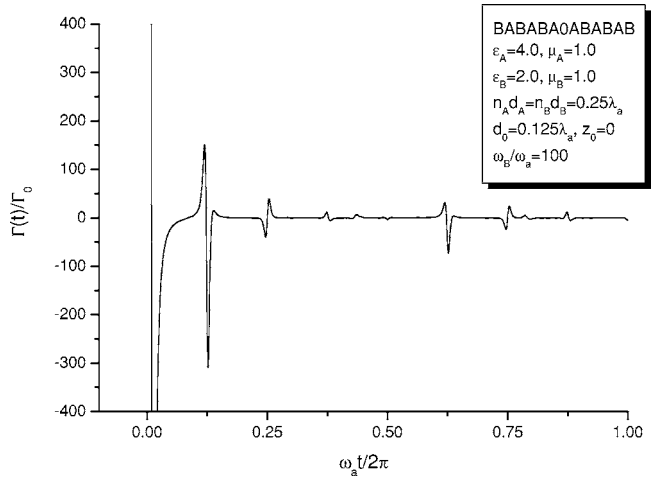

FIG. 10. The SE decay rate in 1DPC with $\varepsilon_A=4.0$, $\mu_A=1.0$, $\varepsilon_B=2.0$, $\mu_B=1.0$, $d_0=\lambda_a/8$, and $n_Ad_A=n_Bd_B=\lambda_a/4$.

fields on the SE decay becomes more evident when the middle layer becomes thin.

In Figs. 12 and 13 we show, respectively, the SE decay and the evolution of $|C_a(t)|^2$ for the case that the 1DPC is the same as in Fig. 3, but the atom is moved to $z_a=3\lambda_a/16$ from $z_a=0$. Now the atom is not located at the center of the middle layer. It is located at the position with a distance $\lambda_a/16$ from the atom to the first interface on the right, and a distance $7\lambda_a/16$ to the first interface on the left. From the figures we see that the first large change of the decay rate occurs at $t=\tau_0/8$, the time that the reflected field comes back to the atom from the first interface on the right side. The second large change of the decay rate occurs at $t=5\tau_0/8$, the time that the reflected field comes back to the atom from the second interface on the right side. The third large change of the decay rate occurs at $t=7\tau_0/8$, the time that the reflected field comes back to the atom from the first interface on the left side.

V. CONCLUSION

In this paper, we have studied the non-Markovian processes in the spontaneous decay of the two-level atom em-

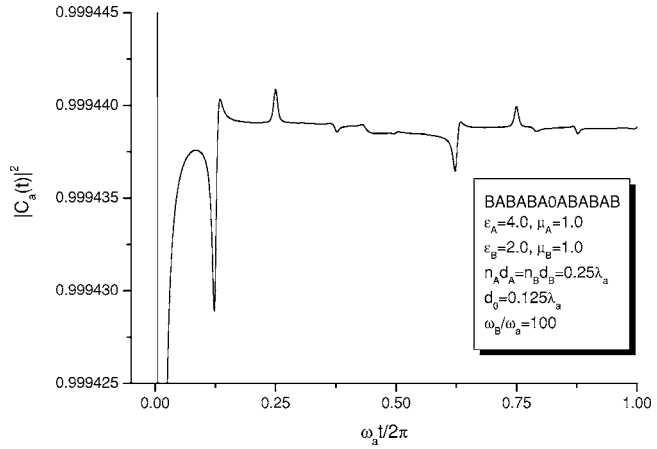

FIG. 11. The evolutions of $|C_a(t)|^2$ in the 1DPC corresponding to Fig. 10.

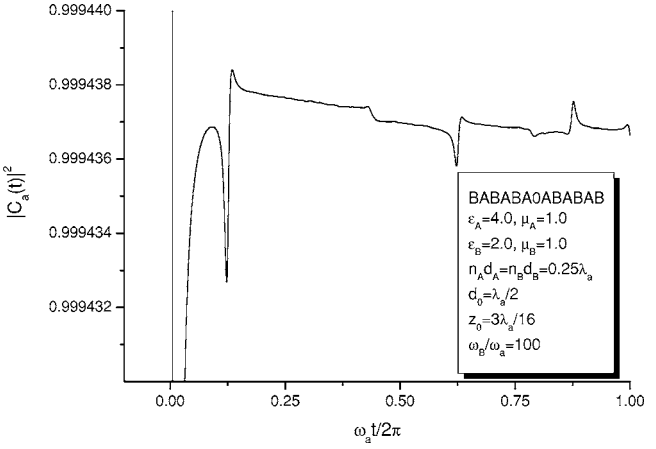

FIG. 12. The SE decay rate in 1DPC with $\varepsilon_A=4.0$, $\mu_A=1.0$, $\varepsilon_B=2.0$, $\mu_B=1.0$, $d_0=\lambda_a/2$, $z_0=3\lambda_a/16$, and $n_Ad_A=n_Bd_B=\lambda_a/4$.

bedded in different 1DPCs. The atomic spontaneous decay is dependent on the interaction of the atom with the field. The total field which drives the atom is a coherent superposition of the multireflected fields. The interference of the multireflected field plays an important role. The field reflected back to the atom can result in constructive interference or destructive interference depending on the structure of the 1DPCs. The SE decay can be enhanced or suppressed with different interference properties. If the interference is constructive, the SE decay is enhanced, while if interference is destructive, the SE decay is suppressed. The steady decay rate after a long time is dependent on the structure of the 1DPC. If the atomic transition frequency corresponds to an allowed normal mode, the steady decay rate is approximately equal to the vacuum decay rate. If the atomic transition frequency is within the forbidden gap, the SE decay is suppressed.

The dynamic non-Markovian processes can be described by a memory function which is dependent on the reservoir coupling spectrum, which is depends on the property of the environment surrounding the atom. In the 1DPCs, the reservoir coupling spectrum is different from that in the vacuum

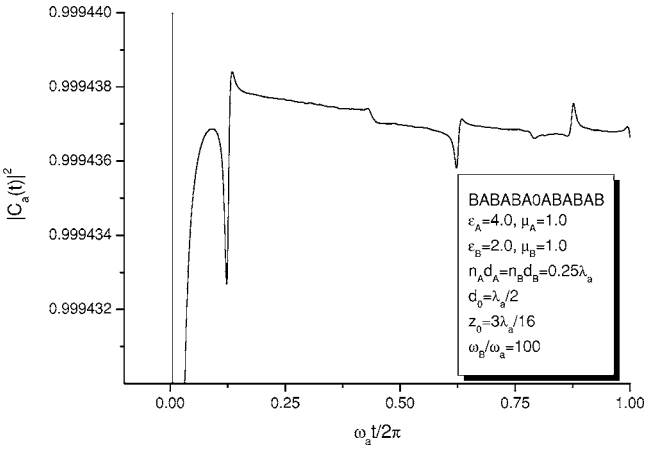

FIG. 13. The evolutions of $|C_a(t)|^2$ in the 1DPC corresponding to Fig. 12.

due to the multireflection. The reservoir coupling spectrum for the 1DPCs oscillates around the reservoir coupling spectrum for the vacuum and leads to some sudden changes on the smooth curve of the memory function in the time domain. The complex memory function governs the dynamic evolution of the atomic spontaneous emission decay.

ACKNOWLEDGMENT

This work was supported by NSFC/05-06/01, the National Natural Science Foundation of China (No. 60268001, No. 90203007), the Phosphor Tracing Plan of Shanghai Science Committee (No. 04QMH1407), and the FRG of HKBU.

[1] M. O. Scully and M. S. Zubairy, Quantum Optics (Cambridge University Press, Cambridge, England, 1997), Chap. 6.
[2] A. G. Kofman and G. Kurizki, Nature (London) **405**, 546 (2000).
[3] P. Facchi, H. Nakazato, and S. Pascazio, Phys. Rev. Lett. **86**, 2699 (2001).
[4] S. De Leo and P. P. Rotelli, Phys. Rev. A **70**, 022101 (2004).
[5] T. Jittoh, S. Matsumoto, J. Sato, Y. Sato, and K. Takeda, Phys. Rev. A **71**, 012109 (2005).
[6] E. Yablonovitch, Phys. Rev. Lett. **58**, 2059 (1987); S. John, *ibid.* **58**, 2486 (1987).
[7] S. John and J. Wang, Phys. Rev. B **43**, 12772 (1991).
[8] S. John and T. Quang, Phys. Rev. Lett. **78**, 1888 (1997).
[9] Shi-Yao Zhu, Yaping Yang, Hong Chen, Hang Zhen, and M. S. Zubairy, Phys. Rev. Lett. **84**, 2136 (2000).
[10] Yaping Yang and Shi-Yao Zhu, Phys. Rev. A **62**, 013805 (2000).
[11] Yaping Yang, M. Fleischhauer, and Shi-Yao Zhu, Phys. Rev. A **68**, 043805 (2003).
[12] Ines de Vega, Daniel Alonso, and Pierre Gaspard, Phys. Rev. A **71**, 023812 (2005).
[13] W. Lukosz, Phys. Rev. B **22**, 3030 (1980).
[14] F. De Martini, M. Marrocco, P. Mataloni, L. Crescentini, and R. Loudon, Phys. Rev. A **43**, 2480 (1991).
[15] S. M. Dutra and P. L. Knight, Phys. Rev. A **53**, 3587 (1996).
[16] H. Rigneault and S. Monneret, Phys. Rev. A **54**, 2356 (1996).
[17] I. Takahashi and K. Ujihara, Phys. Rev. A **56**, 2299 (1997).
[18] Ho Trung Dung and Kikuo Ujihara, Phys. Rev. A **60**, 4067 (1999).
[19] S. Severini, A. Settimi, C. Sibilia, M. Bertolotti, A. Napoli, and A. Messina, Phys. Rev. E **70**, 056614 (2004).
[20] H. J. W. M. Hoekstra and H. B. H. Elrofai, Phys. Rev. E **71**, 046609 (2005).
[21] Jing-Ping Xu, Nian-Hua Liu, and Shi-Yao Zhu, Phys. Rev. E **73**, 016604 (2006).